Phosphinoquinoline supported Co II , Ni II , and Fe II complexes: divergent behaviour upon reduction

Pauline Schiltz, Nicolas Casaretto, Sophie Bourcier, Audrey Auffrant, Corinne Gosmini

Phosphinoquinoline supported Co^{II}, Ni^{II}, and Fe^{II} complexes: divergent behaviour upon reduction

Received 00th January 20xx,
Accepted 00th January 20xx

DOI: 10.1039/x0xx00000x

Pauline Schiltz,[a] Nicolas Casaretto,[a] Sophie Bourcier,[a] Audrey Auffrant,*[a] Corinne Gosmini,*[a]

The reduction of **[CoLBr$_2$]**, a Co^{II} complex supported by a diisopropylphosphinoquinoline (**L**) ligand induced a ligand coupling giving access to a (PNNP) supported Co^{II} complex which was isolated in 70 % yield. That complex was formed using a minimum of two equivalents of reductant (either Mn or KC_8). The fate of **[CoLBr$_2$]** in presence of one equivalent of reductant was more difficult to study nevertheless a Co^{I} complex was characterised in the solid state. In order to determine whether this ligand coupling could occur with other 3d metals, **L** supported Fe^{II}, and Ni^{II} complexes were synthesised. While no compound could be identified upon reduction of **[FeLBr$_2$]**, both **[NiLBr$_2$]** and **[NiL$_2$Br](Br)** led to the reduction at the metal center allowing to isolate in a satisfactory yield an original Ni^0 trimer. This study shows the different behaviour of those 3d metal complexes in the presence of a reductant.

Introduction

Low-valent metals are essential in a variety of stoichiometric[1] and catalytic transformations.[2] In those processes, the key bond-activating and product-forming steps generally rely on an oxidative addition and a reductive elimination step respectively. This has been well-established for palladium catalysed coupling reactions generally involving a Pd^0 catalytic active species.[3]

Considering the common trend to replace scarce and expensive noble metals by cheaper and more abundant 3d elements, the pivotal role of their low valent derivatives has been showed in many different processes (Chart 1a).[2c, 4] In transition metal coupling reactions, Cu, Fe, Ni, and Co catalysts now offer reliable alternatives to Pd.[5]

Co-catalysed coupling processes and particularly the reductive coupling between two electrophiles,[6] requiring the *in situ* reduction of the catalytic intermediate, are our central area of research. This has prompted us to evaluate the potential of mixed ligands for such reductive couplings. As most of the ligands employed for these cobalt-catalysed coupling reactions are either N-heterocycles (pyridine, bipyridine, phenanthroline, quinoline...)[7] or phosphines,[8] we prepared Co^{II} complexes supported by phosphinoquinoline ligands. Allthough such Co complexes were effective for the hydrosilylation of ketones,[9] they were poorly efficient in catalytic reductive coupling reactions. This has stimulated the present study which started by determining the fate of phosphinoquinoline Co complexes in presence of a reductant (Chart 1b).

In this article, we show that the reduction of a phosphinoquinoline cobalt(II) complex led a (PNNP) supported Co^{II} complex resulting from the radical coupling between two N-heterocycles and demonstrated the divergent behaviour of its Fe^{II} and Ni^{II} analogues. Indeed, the latter led to a Ni^0 trimer resulting from a reduction at the metal center.

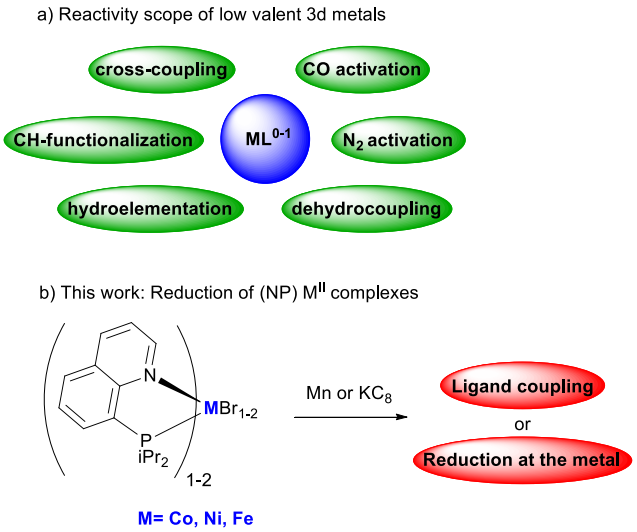

Chart 1: Cross-coupling reactions involving low valent intermediates

Results and discussion

Reduction of L supported Co^{II} complexes.

The reduction of **[CoLBr$_2$]** where **L** is a diisopropylphosphinoquinoline was first conducted in THF with two equivalents of manganese powder at room temperature (Scheme 1). The solution turned from blue to brown. After filtration and removal of the volatiles, the residue was analysed by NMR spectroscopy. The absence of $^{31}P\{^1H\}$ NMR signals and the wide range of chemical shifts observed in the ^1H NMR spectrum (from -12 to 200 ppm see Figure S1) suggested the formation of a paramagnetic complex.

The structure of the formed product was revealed by X-ray diffraction analysis. Crystals were grown by diffusion of pentane into a concentrated dichloromethane solution. The structure presented in Figure 1 shows the formation of a cationic Co^{II} complex exhibiting a tetradentate PNNP ligand (**L^{II}**) which results from the creation of a C-C bond between the carbons α

[a] *Laboratoire de Chimie Moléculaire (LCM), CNRS, Ecole Polytechnique, Institut Polytechnique de Paris Route de Saclay, 91120 Palaiseau, France.*

† Footnotes relating to the title and/or authors should appear here.
Electronic Supplementary Information (ESI) available: [details of any supplementary information available should be included here]. See DOI: 10.1039/x0xx00000x

to the nitrogen atom of the pyridines of the phosphinoquinoline. The charge is balanced by a tribromocobalt anion.

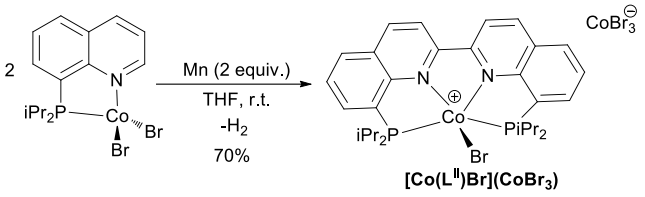

Scheme1: Formation of complex **[Co(L^{II})Br](CoBr$_3$)** upon reduction of **[CoLBr$_2$]**

Even if further investigations would be necessary to understand this transformation, a rearrangement of ligands has occurred allowing a radical coupling between the pyridines and resulting in the formal loss of one H_2. Since **[CoLBr$_2$]** is stable in THF solution at room temperature the exchange of ligands should be triggered by the reduction, which in a first step may affect the metal centre.

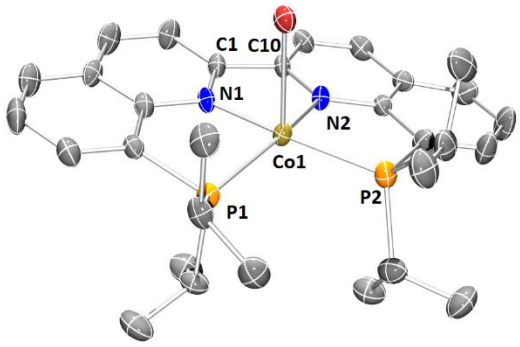

Figure 1: Ortep plot of **[Co(L^{II})Br]$^+$** with thermal ellipsoids (drawn at the 50% probability level). The anion, the H atoms and one CH_2Cl_2 molecule were omitted for clarity. Selected bond lengths [Å] and angles [°]: Co1-N1 1.940(4), Co1-N2 1.933(7), Co1-P1 2.244(2), Co1-P2 2.270(2), Co1-Br1 2.532(2), C1-C10 1.479(9), P1-Co1-N1 83.4(2), P1-Co1-N2 85.0(2), P1-Co1-P2 108.49(9), N1-Co1-N2 80.8(3), N1-Co1-Br1 88.2(2), P1-Co1-Br1 98.21(7), N2-Co1-Br1 97.2(2), P2-Co1-Br1 98.95(7).

The intermolecular coupling of two pyridine rings in presence of low valent metal centres has been already described with lanthanides[10] and 3d-metals such as titanium[11] or iron.[12] In those cases, the electron transfer from the low valent metal to the pyridine ligand induces the formation of the pyridine radical anions which couple. Such reactions were also reported with other pyridine based ligands such as pyrazine[13] or phenantroline[14] but we are not aware of a previous example with quinoline derivatives. Interestingly, recently Werncke and co-workers[12b] studied the reactivity of low valent 3d-metal(I) hexamethyldisilazanides [K(18c6)]M^{I}(N(SiCH$_3$)$_3$)] (M= Cr-Co) with pyridine and showed that all of them led to M^{II} complexes bearing a bridging 4,4'-di-hydrobipyridyl ligand except the cobalt complex.

The NMR proton resonances observed for **[Co(L^{II})Br](CoBr$_3$)** (Figure S1) matched with the observed structure. Four signals with an integration of 2 were seen at -12.1, 14.7, 27.0, and 37.3 ppm as well as two signals at -7.5 and 11.3 integrating for twelve protons each which should correspond to the methyl groups of the isopropyl substituents. In addition, mono- and di-cations [Co(L^{II})]$^{+/+2}$ (m/z 547.1335 and 273.5921 respectively) were observed by HR-mass spectrometry analysis.

In the solid state, **[Co(L^{II})Br]$^+$** exhibits a square based pyramidal geometry (τ_5≈0.12)[15] with the tetradentate ligand occupying the meridional plane and the bromide the apical position. The distance of P1 and Co1 to the P1N1N2 plane was measured respectively at 0.412 and 0.113 Å, both occupying different hemispheres. Co1-Br1 is almost orthogonal to the meridional plane (Br1Co1N2N1 torsion angle 86.99 °) and is elongated (2.532 Å) compared to the bond length observed in **[CoL$_2$Br]$^+$**, in which the N and P atoms were in *trans* position.[9] The Co-N and Co-P bond lengths have not evolved much, but the angles have changed more. The strain due to the coupling led to a narrow N1-Co1-N2 angle (80.8(2)°) and a wide P1-Co1-P2 (108.49(8)°) while in **[CoL$_2$Br]$^+$** all the P-Co-N angles range from 84 to 96°. The bond lengths within the heterocycles have been hardly modified by the bond formation, the created C-C bond measured 1.479(9) which is comparable to one measured in (2,2'-biquinoline)-dibromo-cobalt(II) complex.[16]

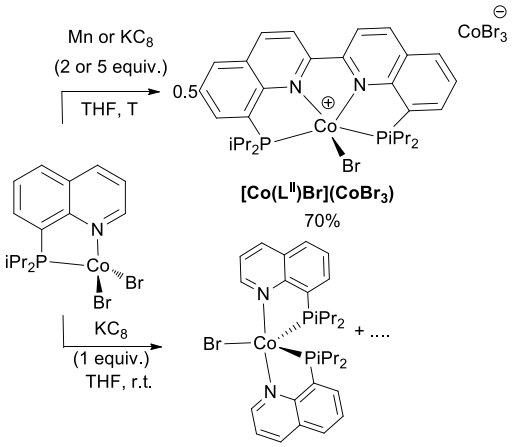

Scheme2: Evolution of **[CoLBr$_2$]** in different reductive conditions

We were curious to determine if the coupling of the ligand would occur with another reductant. We obtained a similar result by adding two equivalents of KC_8 to a THF solution of **[CoLBr$_2$]** previously cooled down to -38°C (Scheme 2). In these conditions **[CoL^{II}Br]** was isolated in 70% yield by crystallisation. The same complex formed also when employing an excess of reductant (5 equivalents of Mn or KC_8).

Employing one equivalent of KC_8 or Mn, led to a colour change of the reaction mixture, however, the crystallisation was much more difficult and we were rarely able to obtain single crystals suitable for X-ray diffraction. We managed once after a reaction with one equivalent of KC_8.

The X-ray structure (Figure 2) shows the formation of a neutral complex resulting from the reduction at the metal centre and a ligand redistribution since two **L** are coordinated to Co. In **[CoL$_2$Br]**, the Co exhibits a trigonal bipyramid geometry (τ_5≈0.91),[15] with the P atoms and the bromide in the meridional plane and the N atoms in apical positions. This differs from the distorted square based pyramid observed for the corresponding cobalt(II) complex **[CoL$_2$Br]$^+$**.[9] The N atoms remain *trans* to each other in the Co^{I} complex. Comparing the bond lengths in **[CoL$_2$Br]** to those in **[CoL$_2$Br]$^+$**; the Co-Br (2.4974(6) vs 2.4385 Å) and the Co-N (2.1841(19) vs 1.983(2) and 1.938(2) Å) bonds

have elongated upon reduction while the Co-P remained similar.

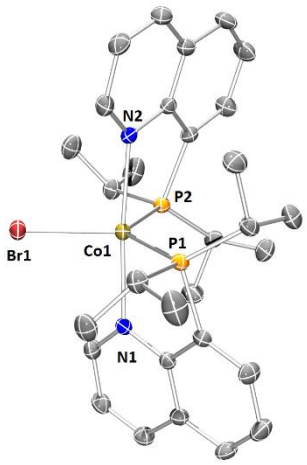

Figure 2: Ortep plot of **[CoL$_2$Br]** with thermal ellipsoids (drawn at the 50% probability level). The H atoms were omitted for clarity. Selected bond lengths [Å] and angles [°]: Co1-N1 = Co-N2 2.184(19), Co1-P1 = Co-P2 2.2741(6), Co1-Br1 2.4971(6), P1-Co1-N1 = P2-Co1-N2 80.32(5), P2-Co1-N1 = P1-Co1-N2 97.11(5), N1-Co1-Br1 = N2-Co1-Br1 92.50(5), P1-Co1-Br1 = P2-Co1-Br1 120.58(18).

The reaction between **[CoL$_2$Br$_2$]** and one equivalent of KC_8 probably formed different compounds, **[CoL$_2$Br]** being one of them. But the formation of Co^{II} and/or Co^0 compounds could not be excluded. Moreover, the very low quantity of **[CoL$_2$Br]** obtained did not allow to test if this complex is an intermediate in the formation of **[Co(L^{II})Br]$^+$**. We also attempted the reduction of **[CoL$_2$Br]** with two equivalents of KC_8 and Mn. In these cases, we only isolated by crystallisation the starting material while the reaction was accompanied by a strong colour change suggesting that a reaction had taken place. Again, we suspect the presence of different products in which Co could have a different oxidation state (0-2), among these the starting material was the most prone to crystallise.

In order to study if the rather unusual coupling of quinoline rings takes place with other 3d metals, we synthetised **L** supported Ni^{II} and Fe^{II} complexes.

Synthesis of L supported Fe^{II} and Ni^{II} complexes.

The coordination of **L** to Ni^{II} was conducted in THF at room temperature using [NiBr$_2$(DME)] as the metal precursor (Scheme 3). After overnight stirring, the volatiles were evaporated and the residue was washed with diethyl ether allowing to isolate **[NiLBr$_2$]** in 89% yield using one equivalent metal precursor and **[NiL$_2$Br](Br)** in 84% yield when employing half equivalent of the Ni^{II} reagent.

These complexes were analysed by NMR spectroscopy, HR-mass spectrometry, and X-ray diffraction analysis. No resonance was observed by $^{31}P\{^1H\}$ NMR spectroscopy while the ^{1}H NMR spectra of both complexes present broad signals pointing to the formation of paramagnetic compounds. The ^{1}H NMR spectrum of **[NiLBr$_2$]** exhibits five signals between 8 and 13 ppm integrating for one proton that should correspond to aromatic protons (one is missing) while the isopropyl methyl groups gave two resonances at 1.74 and 2.58 ppm integrating each for six protons (Figure S2).

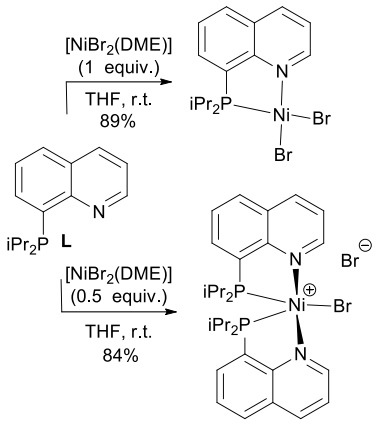

Scheme 3: Synthesis of **[NiLBr$_2$]** and **[NiL$_2$Br](Br)**

The ^{1}H NMR spectrum of **[NiL$_2$Br](Br)** is less well-resolved, it shows signals between -1.5 and 28 ppm whose relative integration was in agreement with the expected number of protons (Figure S3). The magnetic moment of both complexes were measured in solution[17] and values of 0.97 and 0.74 μ_B were obtained for **[NiLBr$_2$]** and **[NiL$_2$Br](Br)** respectively. While Ni^{II} complexes can be diamagnetic when square planar, a higher magnetic moment around 3-3.5 μ_B is expected for a paramagnetic tetrahedral complex. The low values measured are nevertheless not unprecedented, values around 1.3 μ_B were reported for Ni^{II} complexes supported by phosphinopyridine ligand[18] as well as a square planar phosphasalen derivative.[19] These values suggest a distorted geometry in solution.

The structures of both complexes were studied in the solid state. Single red/brown crystals were obtained for **[NiLBr$_2$]** by layering pentane above a dichloromethane solution. The unit cell contains two similar molecules, one is presented in Figure 3 the other one in Figure S11. In this structure, the nickel adopts a distorted square planar geometry (τ_4≈0.12).[20] The coordination bonds measured are slightly shorter (Ni1-P1 2.15366(9), Ni1-N1 1.941(3) Å) than these reported for the cobalt analogue (Co-P 2.3489, Co-N 2.036(2) Å) but this agrees with the small difference of van der Waals radius. Phosphinoquinoline Ni^{II} complexes previously reported in the literature differ from **[NiLBr$_2$]** by the nature of the P substituents (phenyl) and the absence of bromide in the coordination sphere of the metal however they present the same geometry and comparable coordination bonds.[21]

Deep green single crystals were obtained for **[NiL$_2$Br](Br),** their X-ray analysis showed a distorted trigonal bipyramid geometry around the Ni centre (τ_5≈0.71,[15] Figure 3). The bromide Br1 and the phosphorus atoms P1 and P2 form the median containing the nickel while the nitrogen N1 and N2 atoms occupy the apical positions (angle between the two planes 85.49°). The P-Ni1 bonds (2.260(1) and 2.253(1) Å) are slightly longer and the Ni1-N bonds (1.908(4) and 1.922(4) Å) slightly shorted than those measured in **[NiLBr$_2$].**

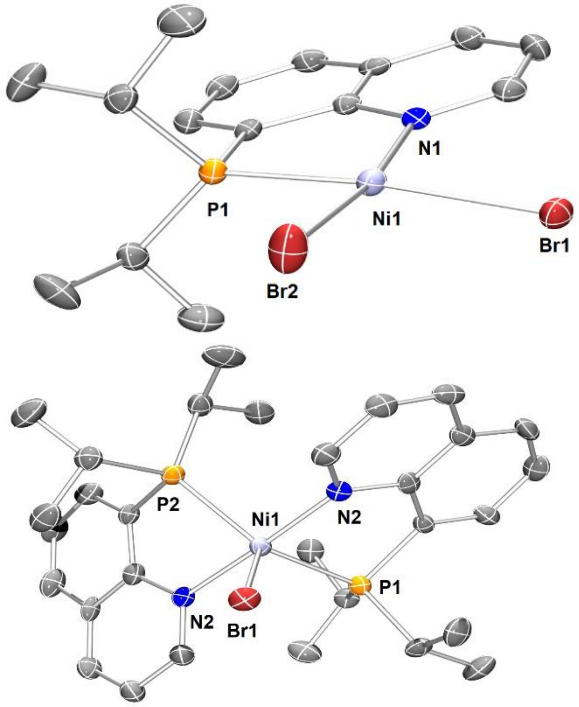

Figure 3: Ortep plot of one molecule **[NiLBr$_2$]** (top) and **[NiL$_2$Br]$^+$** with thermal ellipsoids drawn at the 50% probability level). The H atoms as were omitted for clarity as well as a molecule of CH2Cl2 for . **[NiL$_2$Br]$^+$**. Selected bond lengths [Å] and angles [°]: **[NiLBr$_2$]** Ni1-N1 1.941(3), Ni1-P1 2.1536(9), Ni1-Br1 2.3817(5), Ni1-Br2 2.2908(7), P1-Ni1-N1 83.4(2), P1-Ni1-N2 85.0(2), P1-Ni1-P2 87.62, N1-Ni1-Br1 95.78(8), P1-Ni1-Br2 85.86(3), Br2-Ni1-Br1 91.60(2) ; **[NiL$_2$Br]$^+$** Ni1-N1 1.908(4), Ni1-P1 2.260(1), Ni1-N2 1.922(4), Ni1-P2 2.253(1), Ni1-Br1 2.6218(9), P1-Ni1-N1 85.3(1), P2-Ni1-N2 84.4(1), N1-Ni1-P2 93.2(1), P1-Ni1-N2 94.7(1), N2-Ni1-Br1 92.0(1), P2-Ni1-Br1 114.62(4), N1-Ni1-Br1 91.1(1), P1- Ni1-Br1 111.40(4).

We attempted the synthesis of the corresponding Fe^{II} complexes i.e **[FeLBr$_2$]** and **[FeL$_2$Br]** using a similar strategy (Scheme 4). **L** was reacted with [FeBr$_2$(DME)] in THF at room temperature. The completion of the coordination was ascertained by the disappearance of the P signal of the ligand by *in situ* $^{31}P\{^1H\}$ NMR spectroscopy. Using a 1:1 M:L ratio, the orange solid formed after overnight stirring was identified as **[FeLBr$_2$]** (96% yield) after removal of the volatiles and washing with diethyl ether. This complex was analysed by ^1H NMR spectroscopy and X-ray diffraction.

When the same reaction was conducted with a 1:2 M:L ratio, the $^{31}P\{^1H\}$ NMR spectrum of the reaction mixture after overnight stirring showed the presence of some free ligand. It was separated from the formed complex after washing with diethyl ether and the complex was identified as **[FeLBr$_2$]** (^1H NMR spectroscopy and X-ray crystallography). Using FeBr$_2$ in place of [FeBr$_2$(DME) did not change the outcome of the reaction. The preference to form the 14-electron Fe^{II} complex even in presence of two equivalents of bidentate NP ligand containing the di(isopropyl)phosphine group was previously reported by Kirchner and coworkers with aminophosphinepyridine ligand.[22]

The ^1H NMR spectrum of **[FeLBr$_2$]** in CD_2Cl_2 (Figure S4) shows six broad signals integrating each for one proton between -21 and 183 ppm that should correspond to the quinoline protons as well as two signals integrating for six protons and one for two protons that can be assigned to the isopropyl protons. The magnetic moment of **[FeLBr$_2$]** was measured at 4.99 μ_B in solution indicating a high spin complex with four unpaired electrons.

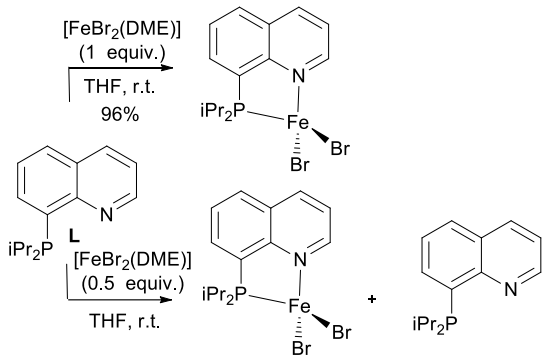

Scheme 4: Coordination of **L** to Fe^{II}

Amber single crystals of **[FeLBr$_2$]** were obtained by slow diffusion of pentane into a concentrated solution of the complex in CH_2Cl_2. The solid-state structure obtained (Figure 4) showed a tetrahedral geometry of the iron cation (τ_4≈0.88).[20]. It resembles that obtained for **[CoLBr$_2$]** however the Fe-N and Fe-P bonds are slightly longer than those observed in the cobalt complex.[9] Herbert and coworkers published the structure of a high spin phosphinophenanthridine Fe^{II} featuring a di(isopropyl)phosphine group. It exhibits a similar geometry with slightly shorter Fe-Br and Fe-P bonds than in **[FeLBr$_2$]** while the Fe-N bonds are similar. [23]

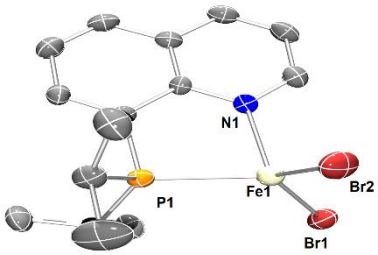

Figure 4: Ortep plot of **[FeLBr$_2$]** with thermal ellipsoids (drawn at the 50% probability level). The H atoms were omitted for clarity. Selected bond lengths [Å] and angles [°]: Fe1-N1 2.115(4), Fe1-P1 2.4488(16), Fe1-Br1 2.4013(10), Fe1-Br2 2.3646(10), N1-Fe1-P1 81.33(11), N1-Fe1-Br1 102.74(11), N1-Fe1-Br2 111.50(12), Br1-Fe1-P1 120.46(5), Br2-Fe1-P1 112.86(5), Br2-Fe1-Br1 119.63(4).

Reduction of L supported Fe^{II} and Ni^{II} complexes.

The reduction of the phosphinoquinoline supported Ni^{II} and Fe^{II} complexes was then studied. As Mn and KC_8 gave similar results with the cobalt complexes, we chose to conduct the reduction with two equivalents of KC_8 in THF at low temperature. Starting from **[FeLBr$_2$]** we observed a strong colour change from orange to black. The obtained solid was analysed by NMR spectroscopy. After reaction, the obtained solid was not silent in $^{31}P\{1H\}$ RMN (resonance at 74.4 ppm, figure S6) and its ^1H NMR spectrum had largely changed: ^1H NMR resonances are observed in the diamagnetic window (Figure S7). This suggest that at least a diamagnetic compound seems to have formed, nevertheless it did not allow to conclude about the structure of the generated complex. Indeed, no crystal could be grown despite numerous attempts.

With the nickel complexes the reaction led to dark brown mixture starting either from **[NiLBr$_2$]** or **[NiL$_2$Br](Br)**. The same light-brown compound formed from these two complexes (Scheme 5) as indicated by $^{31}P\{^1H\}$ NMR spectroscopy showing a singlet at 56.4 ppm (Figure S8). Its ^1H NMR spectrum in THF-d_8 (Figure S9) showed 9 well defined resonances between 0 and

9 ppm.[‡] The signals observed agree with the ligand structure: two doublets of doublets at 0.77 and 1.28 integrating each for six protons were assigned to the methyl protons, the broad septuplet at 2.81 with an integration of 2 to the CH protons, and six well separated aromatic resonances corresponding to the quinoline protons. The latter are only slightly deshielded compared to the free ligand.

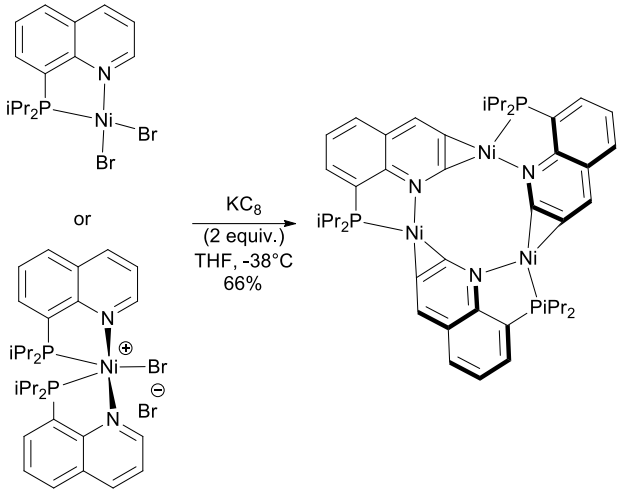

Scheme 5: Reduction of **L** supported Ni^{II} complexes

The structure of this compound was obtained by X-ray diffraction analysis (Figure 5). The single crystals were grown by diffusion of pentane into THF solution. The solid-state structure shows the trimer **[NiL]$_3$** presenting a C3 symmetry, in which each nickel exhibits a rather distorted square planar geometry (τ_4≈0.40).[20]

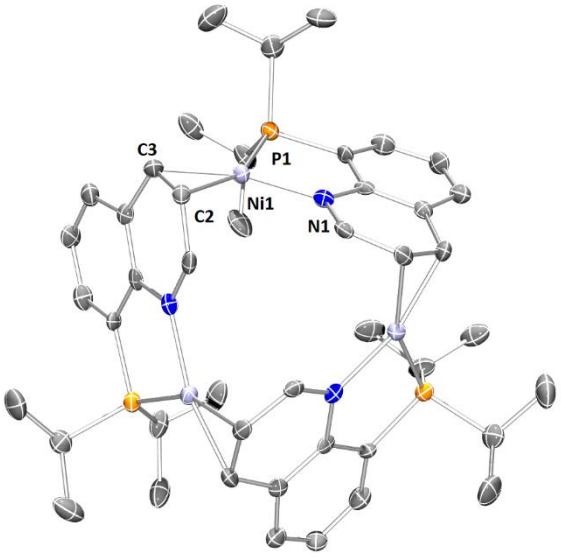

Figure 5: Ortep plot of **[NiL]$_3$** with thermal ellipsoids (drawn at the 50% probability level). The H atoms were omitted for clarity. Selected bond lengths [Å] and angles [°]: Ni1-N1 1.960(7), Ni1-P1 2.150(3), Ni1-C2 1.985(9), Ni1-C3 1.981(8), C2-C3 1.459(12), N1-Fe1-P1 88.7(2), N1-Ni1-C2 115.5(3), C3-Ni1-C2 43.2(3), C3-Ni1-P1 113.0(3)

The nickel is coordinated by the phosphorus and the nitrogen of a quinoline and two carbons of the N-heterocycle of another quinoline ligand in an η^2-mode. The latter is at the origin of the distortion as C2-Ni1-C3 measures 43.2(3)°. The nickel is located in the mean plane defined by the P1,N1, and C2,3 atoms. A 1:1 M:L is observed implying the loss of the bromides and that of one ligand when performing the reaction from **[Ni L$_2$Br](Br)**. In **[NiL$_3$]** the Ni-P and Ni-N measuring respectively 2.150(3) and 1.960(6) Å are comparable to those in **[NiLBr$_2$]**. The length of the metallated C=C bond is important to determine the degree of activation of this bond. It measures 1.459(12) Å, therefore it is elongated compared to that measured in the Ni^{II} complex (1.361(5) Å). Yet this remains much shorter than a C-C single bond pointing towards the η^2-coordination to a Ni^0 centre. Thus, the reaction has led to the reduction of the metal centre affording a diamagnetic Ni^0 16-electron complex. We searched for similar structures in the CCDC and found two examples: Hoberg's group described a nickel(0) dimer with a vinyl pyridine and a triphenylphosphine ligand,[24] while Bernskoetter reported a Ni^0 supported by a tertbutylphosphinomethylpyridine and an η^2-acrylonitrile ligands.[25] They both showed a square planar geometry with Ni-P, Ni-N, and η^2-CC bond lengths in the same range as those measured for **[NiL]$_3$**. Having established the structure of the formed product, the yield of the reduction was determined: **[NiL]$_3$** was obtained in 66% from **[NiLBr$_2$]**. Contrary to what was observed with cobalt no coupling of quinoline ligand was observed, a trimer resulting from the reduction at the metal centre was formed pretty efficiently.

Conclusions

We showed that the reduction of a phosphinoquinoline supported cobalt(II) complex with two equivalents of reductant (Mn, or KC_8) led to a rather unusual C-C coupling between two ligand allowing to isolate in a good yield a Co^{II} complex featuring an almost planar PNNP tetradentate ligand. The analogous nickel(II) and iron(II) complexes were synthesised to investigate whether the same reaction takes place. The **[FeLBr$_2$]** was characterised as a high spin tetrahedral complex (S=2) while both nickel complexes **[NiLBr$_2$]** or **[NiL$_2$Br]** exhibit a low magnetic moment in solution as a probable consequence of a distorted geometry in solution. While we got little information regarding the reduction of the Fe^{II} complexes, that of the Ni^{II} derivatives led to a rather rare trimeric Ni^0 complex resulting from the reduction at the metal centre. In **[NiL$_3$]**, the nickel is chelated by the N and P atoms of a phosphinoquinoline ligand and two carbons belonging to the N-heterocycle of another ligand and exhibits a square planar geometry. This study underlines the divergent behaviour of similar complexes depending on the nature of the metal centres. Both types of reduction products will require further investigations. On the one hand, the reactivity of the resulting Co^{II} complex should be studied. In particular if conditions could be found for an efficient demetallation, it would open an avenue to study the coordination chemistry of an original PNNP tetradentate ligand that has yet no equivalent in the literature. On the other hand, the isolated Ni^0 trimer should present an interesting reactivity and would be interesting to investigate in the context of coupling reactions and/or activation of small molecules.

Experimental Part

All air and moisture sensitive reactions were performed under inert atmosphere using a vacuum line, inert Schlenk techniques (N_2) and a glove box (Ar, <0.1 ppm H_2O, <0.1 ppm O_2) with oven-dried glassware unless other notified. **[CoLBr$_2$]**[9] and KC_8[26] were synthesised as previously reported while all other reagents were used as received from commercially available suppliers without further purification unless otherwise noticed. The temperature of -38°C corresponds to that of freezer of the glovebox. CH_2Cl_2, pentane, ether and toluene were taken from solvent purification system (MBraun-SPS). THF was distilled and degassed using freeze-pump technique. CD_2Cl_2 was degassed using freeze-pump technique. NMR spectra were recorded on a Bruker AC-300 SY spectrometer at 300 MHz for ^{1}H and 121.5 MHz for ^{31}P. Solvent peaks were used as internal references for ^{1}H while ^{31}P{^{1}H} NMR spectra are relative to an 85% H_3PO_4 external reference. Unless otherwise mentioned, NMR spectra were recorded at 300 K. Coupling constant are expressed in hertz. The following abbreviations are used: br, broad; s, singlet; d, doublet; q: quadruplet; t, triplet; m, multiplet; v, virtual. Full Width Half Maximum (FWHF) is indicated in hertz. The spectra were analysed with MestReNova software. Mass spectrometry experiments were performed on a Tims-TOF mass spectrometer (Bruker, France). Electrospray source has been used in positive and negative modes. Samples are prepared in acetonitrile with 0.1 % formic acid at µM concentration. 2 to 10 µL were introduced without separation with Elute UHPLC module (Bruker) at a 100 µL min^{-1} flow rate into the interface of the instrument. Capillary and end plate voltages were set at 4.5 kV and 0.5 kV for ESI experiments. Nitrogen was used as the nebuliser and drying gas at 2 bar and 8 L min^{-1}, respectively, with a drying temperature of 220 °C for ESI source. Tuning mix (Agilent, France) was used for calibration. The elemental compositions of all ions were determined with the instrument software Data Analysis, the precision of mass measurement was less than 3 ppm. X-ray crystallography data were collected at 150 K on a Bruker Kappa APEX II diffractometer using a Mo-κ (λ=0.71069Å) X-ray source and a graphite monochromator. The crystal structures were solved using Shelxt[27] or olex[28] and refined using Shelxl-97 or Shelxl-2014.[27] ORTEP drawings were made using ORTEP III[29] for Windows. Details of crystal data and structure refinements are summarised in tables S1-2

Synthesis of [Co(L^{II})Br](CoBr$_3$): KC_8 (135 mg, 1 mmol, 2 equiv.) was added to a cold solution of complex **[CoLBr$_2$]** (232 mg, 0.5 mmol, 1 equiv.) in THF (6 mL). The mixture was kept at -38 °C overnight without stirring. Colour changed to deep dark brown mixture. After filtration, volatiles were removed under vacuum and CH_2Cl_2 (4 mL) was added. After filtration, volatiles were removed under vacuum leading to **[Co(L^{II})Br](CoBr$_3$)** as a black shiny solid (162 mg, 0.175 mmol, 70%). Single crystals were grown in CH_2Cl_2/pentane layering at room temperature and afforded black crystals. ^{1}H NMR (THF-d$_8$): δ 200.56 (br. s, FWHM= 9.2 Hz, 4H), 37.32 (br. s, FWHM= 11.4 Hz, 2H,) 26.96 (br. s,FWHM= 11.4 Hz, 2H), 14.69 (br. s,FWHM= 16.0 Hz, 2H), 11.28 (br. s,FWHM= 58.5 Hz, 12H), -7.46 (br. s,FWHM= 22.9 Hz, 12H), -12.07 (br. s,FWHM= 9.2 Hz2H). Evans method (C = 0.012 mM, CD_2Cl_2) μ_{eff}: 4.58 μ_B. HR-MS (ESI$^+$): calculated for $[C_{30}H_{38}N_2CoP_2]^+$ ([M-Br]$^+$) 547.1837; found 547.1835.

Synthesis of [NiLBr$_2$]: A solution of **L** (245 mg, 1 mmol, 1 equiv.) in THF (10 mL) was introduced by cannula to a purple suspension of [$NiBr_2$(DME)] (313 mg, 0.5 mmol, 1 equiv.) in THF (10 mL) at room temperature. The mixture was stirred at room temperature overnight. Volatiles were removed under vacuum and the orange solid was washed with diethyl ether (4 x 5 mL). After drying, **[NiLBr$_2$]** was obtained as a maroon solid (412 mg, 0.89 mmol, 89%). Single crystals were grown in CH_2Cl_2/pentane layering at room temperature and afforded red/brown crystals. ^{1}H NMR (CD_2Cl_2): δ 12.50 (br. s,FWHM= 17.2 Hz, 1H), 10.76 (br. s,FWHM= 35.6 Hz, 1H), 10.05 (br. s,FWHM= 35.2 Hz, 1H), 9.60 (br. s,FWHM= 25.6 Hz, 1H), 8.49 (br. s,FWHM= 23.7 Hz, 1H), 2.58 (br. s,FWHM= 21.3 Hz, 6H), 1.74 (br. s,FWHM= 19.0 Hz, 6H). Evans method (C = 0.029 mM, CD_2Cl_2) μ_{eff}: 0.97 μ_B.HR-MS (ESI$^+$): calculated for $[C_{15}H_{20}BrNNiP]^+$ ([M-Br]$^+$) 381.9865; found 381.9860.

Synthesis of [NiL$_2$Br](Br): The procedure is similar as for complex **[NiLBr$_2$]**. **L** (293 mg, 1.1 mmol, 2.1 equiv.) and [$NiBr_2$(DME)] (160 mg, 0.5 mmol, 1 equiv.) in THF (15 mL) were reacted. **[L$_2$NiBr](Br)** was obtained as a green forest solid (309 mg, 0.44 mmol, 84%). Single crystals were grown in CH_2Cl_2/pentane layering at room temperature and afforded deep green crystals. ^{1}H NMR (CD_2Cl_2): δ 27.66 (br. s,FWHM= 16.0 Hz, 2H,), 18.54 (br. s, FWHM= 38.9 Hz, 2H), 12.48 (br. s, FWHM= 13.7 Hz, 2H), 11,46 (br. s, FWHM= 67.3 Hz, 2H), 11.06 (br. s, FWHM= 66.5 Hz, 2H), 10.73 (br. s, FWHM= 50.4 Hz, 2H), 9.80 (m, FWHM= 6.9 Hz, 10H), 8.44 (br. s, FWHM= 30.8 Hz, 2H), 2.56 (br. s,FWHM= 31.1 Hz, 10H), -1.14 (6H, br. s,FWHM= 108.7 Hz). Evans method (C = 0.029 mM, CD_2Cl_2) μ_{eff}: 0.94 μ_B. HR-MS (ESI$^+$): calculated for $[C_{30}H_{40}BrN_2NiP_2]^+$ ([M-Br]$^+$) 627.1198; found 627.1201.

Synthesis of [FeLBr$_2$]: A solution of **L** (245 mg, 1 mmol, 1 equiv.) in THF (10 mL) was introduced by cannula to a brown solution of [$FeBr_2$(DME)] (310 mg, 0.5 mmol, 1 equiv.) in THF (10 mL) at room temperature. The mixture was stirred at room temperature overnight. Volatiles were removed under vacuum and the orange solid was washed with ether (4 x 5 mL). After drying, **[FeLBr$_2$]** was obtained as an orange solid (443 mg, 0.96 mmol, 96%). Single crystals were grown in CH_2Cl_2/pentane layering at room temperature and afforded amber crystals. ^{1}H NMR (CD_2Cl_2): δ 182.67 (br. s,FWHM= 6.9 Hz, 1H), 42.48 (br. s,FWHM= 20.6 Hz, 1H), 24.08 (br. s,FWHM= 65.2 Hz, 1H), 19.36 (br. s,FWHM= 20.6 Hz, 1H), 14.38 (br. s,FWHM= 65.0 Hz, 1H), 9.65 (br. s,18.3 Hz, 6H), 7.68 (br. s,FWHM= 11.4 Hz, 2H), -5.02 (br. s,FWHM= 13.7 Hz, 2H), -21.01(br. s,FWHM= 77.2 Hz, 1H). Evans method (C = 0.026 mM, CD_2Cl_2) μ_{eff}: 4.99 μ_B, S = 2. Anal. Calcd for $C_{15}H_{20}Br_2FeNP.01\ C_5H_{12}$: C, 39.76; H, 4.56; N, 2.99. Found: C, 39.68; H, 4.40; N, 3.02.

Synthesis of [NiL]$_3$: KC_8 (27 mg, 0.2 mmol, 2 equiv.) was added to a cold solution of **[LNiBr$_2$]** (46 mg, 0.1 mmol, 1 equiv.) in THF (8 mL). The mixture was kept at -38 °C overnight without stirring. Colour changed to deep dark brown mixture. After filtration, volatiles were removed under vacuum and the brown residue was scratched with pentane (2 mL). After drying, a pale brown solid was obtained leading to **[NiL]$_3$** (20 mg, 0.022 mmol, 66%). ^{31}P{H} NMR (THF-d$_8$): δ 56.4 (s) ppm.^{1}H NMR (THF-d$_8$): δ 8.88 (d, $J_{H,H}$= 2.5 Hz, 1H), 8.48 (dd, $J_{H,H}$= 7.5 Hz, $J_{P,H}$= 12.5 Hz, 1H), 8.32 (d, $J_{H,H}$= 8.0 Hz, 1H), 8.04 (d, $J_{H,H}$= 8.0 Hz, 1H), 7.68 (t, $J_{H,H}$=

7.5 Hz, 1H), 7.50 (m, 1H), 2.82 (dq, $J_{H,H}$= 7.5 Hz, $J_{P,H}$ =14.5 Hz, 2H), 1.29 (dd, $J_{H,H}$= 7.0 Hz, $J_{P,H}$ = 15.0 Hz, 6H), 0.77 (dd, $J_{H,H}$= 7.0 Hz, $J_{P,H}$ = 16.0 Hz, 6H). ^{13}C NMR (THF-d_8): 149.6 (s, CH); 137.6 (d, $J_{P,C}$= 4.5 Hz, C), 136.5 (d, $J_{P,C}$= 2.5 Hz, CH), 136.3 (s, C), 131.3 (d, $J_{P,C}$= 3.0 Hz, CH), 130.3 (s, CH), 125.9 (d, $J_{P,C}$= 10.5 Hz, CH), 121.2 (s, CH), 27.6 (d, $J_{P,C}$= 67.5 Hz, CH), 16.6 (d, $J_{P,C}$= 2.5 Hz, CH_3), 15.7 (d, $J_{P,C}$= 3.0 Hz, CH_3).

Conflicts of interest

There are no conflicts to declare.

Acknowledgements

CNRS and Ecole polytechnique are thanked for financial support.

Notes and references

‡ Given the low solubility of [NiL_3] in THF, ^{1}H high quality spectra were only obtained after carefully setting of a saturated THF-d_8 solution of the complex, otherwise the observed resonances are pretty broad.

1. a) M. P. Shaver and M. D. Fryzuk, *Adv. Synth. Catal.*, 2003, **345**, 1061-1076; b) X. Hu, I. Castro-Rodriguez and K. Meyer, *J. Am. Chem. Soc.*, 2004, **126**, 13464-13473; c) M. D. Walter, in *Advances in organometallic Chemistry*, ed. P. J. Perez, 2016, vol. 65, pp. 261-377; d) Z. L. Huang, M. Rafiq, A. R. Woldu, Q. X. Tong, D. Astruc and L. S. Hu, *Coord. Chem. Rev.*, 2023, **478**.

2. a) J. Hartwig, ed., *Organotransition Metal Chemistry: From Bonding to Catalysis*, University Science books, 2009; b) E. P. Beaumier, A. J. Pearce, X. Y. See and I. A. Tonks, *Nat. Rev. Chem.*, 2019, **3**, 15-34; c) L. J. Taylor and D. L. Kays, *Dalton Trans.*, 2019, **48**, 12365-12381.

3. F. D. Armin de Meijere, ed., *Metal-Catalyzed Cross-Coupling Reactions*, Wiley-VCH, 2004.

4. a) E. Nakamura and N. Yoshikai, *J. Org. Chem.*, 2010, **75**, 6061-6067; b) K. Gao and N. Yoshikai, *Acc. Chem. Res.*, 2014, **47**, 1208-1219; c) J. A. Garduño, A. Arévalo and J. J. García, *Dalton Trans.*, 2015, **44**, 13419-13438; d) F. Kreyenschmidt, S. E. Meurer and K. Koszinowski, *Chem. Eur. J.*, 2019, **25**, 5912-5921; e) C. Dorval and C. Gosmini, in *Cobalt Catalysis in Organic Synthesis*, 2020, pp. 163-205; f) S. H. Kyne, G. Lefèvre, C. Ollivier, M. Petit, V.-A. Ramis Cladera and L. Fensterbank, *Chem. Soc. Rev.*, 2020, **49**, 8501-8542; g) V. T. Tran, Z.-Q. Li, O. Apolinar, J. Derosa, M. V. Joannou, S. R. Wisniewski, M. D. Eastgate and K. M. Engle, *Angew. Chem. Int. Ed.*, 2020, **59**, 7409-7413; h) A. Bismuto, P. Müller, P. Finkelstein, N. Trapp, G. Jeschke and B. Morandi, *J. Am. Chem. Soc.*, 2021, **143**, 10642-10648.

5. a) K. S. M. Salih, *Asian J. Org. Chem.*, 2022, **11**, e202200023; b) T. Shu and J. Cossy, *Chem. Eur. J.*, 2021, **27**, 11021-11029; c) K. Juhász, Á. Magyar and Z. Hell, *Synthesis*, 2021, **53**, 983-1002; d) R. Jana, T. P. Pathak and M. S. Sigman, *Chem. Rev.*, 2011, **111**, 1417-1492; e) C. Gosmini and A. Moncomble, *Isr. J. Chem.*, 2010, **50**, 568-576.

6. C. E. I. Knappke, S. Grupe, D. Gärtner, M. Corpet, C. Gosmini and A. Jacobi von Wangelin, *Chem. Eur. J.*, 2014, **20**, 6828-6842.

7. a) O. M. Kuzmina, A. K. Steib, J. T. Markiewicz, D. Flubacher and P. Knochel, *Angew. Chem. Int. Ed.*, 2013, **52**, 4945-4949; b) M. Corpet, X.-Z. Bai and C. Gosmini, *Adv. Synth. Catal.*, 2014, **356**, 2937-2942; c) A. D. Benischke, I. Knoll, A. Rérat, C. Gosmini and P. Knochel, *Chem. Commun.*, 2016, **52**, 3171-3174; d) C. Dorval, M. Tricoire, J.-M. Begouin, V. Gandon and C. Gosmini, *ACS Catal.*, 2020, **10**, 12819-12827; e) F. H. Lutter, L. Grokenberger, P. Spieß, J. M. Hammann, K. Karaghiosoff and P. Knochel, *Angew. Chem. Int. Ed.*, 2020, **59**, 5546-5550.

8. a) M. Amatore and C. Gosmini, *Chem. Eur. J.*, 2010, **16**, 5848-5852; b) Y. Cai, A. D. Benischke, P. Knochel and C. Gosmini, *Chem. Eur. J.*, 2017, **23**, 250-253; c) R. Cheng, G. de Ruiter and C.-J. Li, *Chem. Commun.*, 2022, **58**, 11563-11566.

9. P. Schiltz, N. Casaretto, A. Auffrant and C. Gosmini, *Chem. Eur. J.*, 2022, **28**.

10. a) I. L. Fedushkin, V. I. Nevodchikov, M. N. Bochkarev, S. Dechert and H. Schumann, *Russ. Chem. Bull.*, 2003, **52**, 154-159; b) F. Jaroschik, F. Nief, X.-F. Le Goff and L. Ricard, *Organometallics*, 2007, **26**, 3552-3558; c) W. Huang, S. I. Khan and P. L. Diaconescu, *J. Am. Chem. Soc.*, 2011, **133**, 10410-10413; d) S. Labouille, F. Nief, X.-F. Le Goff, L. Maron, D. R. Kindra, H. L. Houghton, J. W. Ziller and W. J. Evans, *Organometallics*, 2012, **31**, 5196-5203; e) T. Cheisson, L. Ricard, F. W. Heinemann, K. Meyer, A. Auffrant and G. Nocton, *Inorg. Chem.*, 2018, **57**, 9230-9240.

11. a) L. D. Durfee, P. E. Fanwick, I. P. Rothwell, K. Folting and J. C. Huffman, *J. Am. Chem. Soc.*, 1987, **109**, 4720-4722; b) J. R. Aguilar-Calderón, J. Murillo, A. Gomez-Torres, C. Saucedo, A. Jordan, A. J. Metta-Magaña, M. Pink and S. Fortier, *Organometallics*, 2020, **39**, 295-311.

12. a) T. R. Dugan, E. Bill, K. C. MacLeod, G. J. Christian, R. E. Cowley, W. W. Brennessel, S. Ye, F. Neese and P. L. Holland, *J. Am. Chem. Soc.*, 2012, **134**, 20352-20364; b) I. Müller and C. G. Werncke, *Chem. Eur. J.*, 2021, **27**, 4932-4938.

13. W. J. Evans and D. K. Drummond, *J. Am. Chem. Soc.*, 1989, **111**, 3329-3335.

14. G. Nocton, W. W. Lukens, C. H. Booth, S. S. Rozenel, S. A. Medling, L. Maron and R. A. Andersen, *J. Am. Chem. Soc.*, 2014, **136**, 8626-8641.

15. A. W. Addison, T. N. Rao, J. Reedijk, J. van Rijn and G. C. Verschoor, *J. Chem. Soc. Dalton Trans.*, 1984, 1349-1356.

16. L. Smolko, J. Černák, M. Dušek, J. Miklovič, J. Titiš and R. Boča, *Dalton Trans.*, 2015, **44**, 17565-17571.

17. E. M. Schubert, *J. Chem. Educ.*, 1992, **69**, 62.

18. F. Speiser, P. Braunstein and L. Saussine, *Organometallics*, 2004, **23**, 2625-2632.

19. T. P. A. Cao, S. Labouille, A. Auffrant, Y. Jean, X. F. Le Goff and P. Le Floch, *Dalton Trans.*, 2011, **40**, 10029-10037.

20. L. Yang, D. R. Powell and R. P. Houser, *Dalton Trans.*, 2007, 955-964.

21. a) M. Mori, Y. Sunatsuki and T. Suzuki, *Inorg. Chem.*, 2020, **59**, 18225-18240; b) A. Hashimoto, H. Yamaguchi, T. Suzuki, K. Kashiwabara, M. Kojima and H. D. Takagi, *Eur. J. Inorg. Chem.*, 2010, **2010**, 39-47; c) W.-H. Sun, Z. Li, H. Hu, B. Wu, H. Yang, N. Zhu, X. Leng and H. Wang, *New J. Chem.*, 2002, **26**, 1474-1478.

22. a) C. Holzhacker, C. M. Standfest-Hauser, M. Puchberger, K. Mereiter, L. F. Veiros, M. J. Calhorda, M. D. Carvalho, L. P. Ferreira, M. Godinho, F. Hartl and K. Kirchner, *Organometallics*, 2011, **30**,

6587-6601; b) C. Holzhacker, M. J. Calhorda, A. Gil, M. D. Carvalho, L. P. Ferreira, B. Stöger, K. Mereiter, M. Weil, D. Müller, P. Weinberger, E. Pittenauer, G. Allmaier and K. Kirchner, *Dalton Trans.*, 2014, **43**, 11152-11164.
23. R. Mondal, J. D. Braun, I. B. Lozada, R. Nickel, J. van Lierop and D. E. Herbert, *New J. Chem.*, 2021, **45**, 4427-4436.
24. H. Hoberg, D. Guhl and P. Betz, *J. Organomet. Chem.*, 1990, **387**, 233-246.
25. Z. R. Greenburg, D. Jin, P. G. Williard and W. H. Bernskoetter, *Dalton Trans.*, 2014, **43**, 15990-15996.
26. a) D. E. Bergbreiter and J. M. Killough, *J. Am. Chem. Soc.*, 1978, **100**, 2126-2134; b) J. M. Lalancette, G. Rollin and P. Dumas, *Can. J. Chem.*, 1972, **50**, 3058-3062.
27. G. Sheldrick, *Acta Crystallogr. A*, 2015, **71**, 3-8.
28. O. V. Dolomanov, L. J. Bourhis, R. J. Gildea, J. A. K. Howard and H. Puschmann, *J. Appl. Crystallogr.*, 2009, **42**, 339-341.
29. L. J. Farrugia, Department of Chemistry, University of Glasgow, 2001.